

## Effect of stress on the passivation of Si-DLC coating as stent materials in simulated body environment

N.D. Nam<sup>a</sup>, S.H. Lee<sup>a</sup>, J.G. Kim<sup>a,\*</sup>, J.W. Yi<sup>b</sup>, K.R. Lee<sup>b</sup>

<sup>a</sup> Department of Advanced Materials Engineering, Sungkyunkwan University 300 Chunchun-Dong, Jangan-Gu, Suwon 440-746, Republic of Korea

<sup>b</sup> Future Technology Research Division, Korea Institute of Science and Technology, P.O. Box 131, Cheongryang, Sungbuk-Gu, Seoul 130-650, Republic of Korea

### ARTICLE INFO

#### Article history:

Received 19 November 2008

Received in revised form 25 February 2009

Accepted 26 February 2009

Available online 9 March 2009

#### Keywords:

Diamond-like carbon

Sputtering

Corrosion

Strain

Biomaterials

### ABSTRACT

DLC coating can be used for vascular stents to prevent the stainless steel substrate from eluting Ni and Cr by plastic deformation and corrosion environment. The stress corrosion cracking (SCC) of Si-diamond-like carbon (Si-DLC) coated on 316L stainless steel was studied in a simulated body environment of a deaerated 0.89 wt.% NaCl electrolyte at 37 °C. This paper investigated the effect of Si-DLC coating on the SCC of 316L SS by slow-strain-rate test (SSRT), constant load test (CLT), and electrochemical impedance spectroscopy (EIS). The EIS data were monitored for the elastic and plastic regions under CLT to determine the electrochemical behavior of the passive film during SCC phenomena. The Si-DLC coated steel exhibited more ductility than uncoated steel and less susceptibility to SCC in this environment. According to X-ray photoelectron spectroscopy (XPS) analysis, the film repassivation occurs due to the presence of the silicon oxide layer on the Si-DLC film surface.

© 2009 Elsevier B.V. All rights reserved.

### 1. Introduction

Vascular stents are devices used in coronary angioplasty, a medical practice that decreases restenosis following vessel lesions [1]. The main characteristics of stents, which are made from materials able to fulfill precise mechanical properties, are the ability to expand when deployed and to preserve this expansion against the pressure exerted by the vessel wall [2]. Stents can keep blood flowing smoothly through diseased and/or damaged blood vessels during and after vascular surgery, which is a procedure that uses an inflated balloon to enlarge the vessel [3]. However, stent materials are often compromised by two adverse effects [4], corrosion and stress: (1) Corrosion is unavoidable because the body is an aqueous medium containing various ions and organic substances, forming an electrolyte solution [5–10]. These ions react electrochemically with the surface of metallic biomaterials to cause corrosion. (2) Stents are exposed to two main stresses: the first due to the contact with blood vessel and the second being the shear stress provoked by the blood flow and pressure required by stents to expand [11–16]. In the field of biomaterials, SCC is particularly insidious for biomaterials devices that are subjected to mechanical stress in a biological environment rich in chlorides [2]. To inhibit effectively the multilevel interconnection from stress-related corrosion malfunction, the SCC problem of stent materials needs to be examined. Three conditions are considered to be required simulta-

neously to produce SCC: a critical environment, a susceptible alloy, and some component of tensile stress [17]. One of the most commonly applied methods used for SCC testing is the use of a constantly applied tensile load to act as a driving force to induce SCC. A loading device such as a proof ring was used for testing in order to determine the load needed to deflect the ring to the desired value. The operation of the proof ring was based on the ability to transfer the load of a deflected proof ring to a tensile specimen to obtain a constant, sustained loading of the test specimen. While under constant load, the material being evaluated was exposed to a corrosive environment.

The stress corrosion cracks have been detected by the electrochemical impedance spectroscopy measurement [18–21]. However, very few investigations have used electrochemical impedance spectroscopy (EIS) to study repassivation of films [22]. EIS is a sensitive and nondestructive method which enables impedance parameters to be evaluated as a function of time and used to appraise the film's breakdown and passivation.

Diamond-like carbon (DLC) coated on 316L SS has been widely applied in the manufacture of vascular stents. Furthermore, to prevent elution of Ni and Cr, the DLC coatings on vascular stents need to be capable of surviving the plastic deformation of the stainless steel substrate (SS) [23]. Under suitable condition, DLC coatings on SS exhibit excellent properties such as corrosion resistance, electric insulation, low friction, high wear resistance, biocompatibility and high elastic property [24–27]. In the present paper, stress corrosion tests were conducted to obtain a better understanding of how stress affects the passivation of stent materials. This study focuses on the

\* Corresponding author. Tel.: +82 312907360; fax: + 82 312907371.

E-mail address: [kimjg@skku.ac.kr](mailto:kimjg@skku.ac.kr) (J.G. Kim).

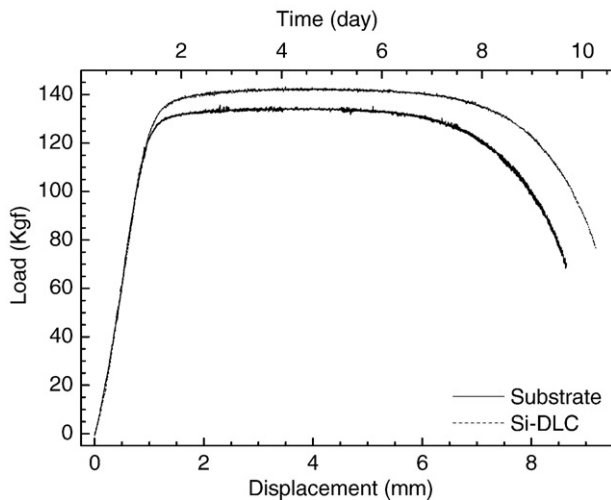


Fig. 1. Stress–strain–time curves of 316L SS and Si-DLC coated on 316L SS at  $10^{-6} \text{ s}^{-1}$  strain rate in 0.89 wt.% NaCl electrolyte deaerated by bubbling high purity nitrogen gas at 37 °C.

effect of stress on the passivation of Si-DLC coatings as material candidates for vascular stents.

## 2. Materials and methods

### 2.1. Materials preparation

Type 316L SS was used as the substrate material. Cylindrical specimens of the SS substrate were fabricated according to NACE standard TM 0177-96 [28], and had threaded ends with 1/4 in. diameter and 1 in. gauge length. Sample surfaces were mechanically polished down to an average roughness of  $R_a \approx 0.1 \mu\text{m}$  using SiC paper and diamond paste. Si-DLC films were prepared by radio frequency plasma-assisted, chemical vapor deposition (RF-PACVD). The substrate was placed on the water-cooled cathode to which 13.56 MHz rf power was delivered through the impedance-matching network. Before deposition, the substrates were cleaned using argon ion for 30 min at 6 sccm, with a bias voltage of  $-750 \text{ Vb}$  and pressure of  $3.7 \times 10^{-3} \text{ Torr}$ . The precursor gases used for Si-interlayer (Si buffer) and Si-DLC films were silane ( $\text{SiH}_4$ ,  $\text{SiH}_4:\text{H}_2 = 10:90$ ) and a mixture of  $\text{C}_6\text{H}_6$  and silane, respectively. The vacuum vessel was pumped to a base pressure of approximately  $2.4 \times 10^{-5} \text{ Torr}$  prior to deposition. A Si buffer was used for the Si interlayer at  $-400 \text{ Vb}$  with silane of 5 sccm and a pressure of  $10 \times 10^{-3} \text{ Torr}$ . An approximately 0.01- $\mu\text{m}$ -thick Si interlayer was deposited onto the substrate, and then Si-DLC films of a 1- $\mu\text{m}$ -thick were deposited with a mixture gases of  $\text{C}_6\text{H}_6$  (3.2 sccm) and silane (3 sccm) at  $-400 \text{ Vb}$  and a pressure of  $10 \times 10^{-3} \text{ Torr}$ .

### 2.2. Slow-strain-rate test (SSRT)

The specimen for the slow-strain-rate test (SSRT) was coated with an insulating lacquer to give an identical, exposed surface area. The tensile test specimen was installed in the test cell so that the entire gauge length of the specimen was immersed in the solution. The specimen was connected to the pull-rods, and the load and elongation

Table 1

SSRT results for 316L SS and Si-DLC coated on 316L SS at a strain rate of  $10^{-6} \text{ s}^{-1}$  in deaerated 0.89 wt.% NaCl electrolyte at body temperature of 37 °C.

Specimen	Time to fracture (day)	Elongation (%)	Yield stress (kgf/mm <sup>2</sup> )	Fracture stress (kgf/mm <sup>2</sup> )
316L SS	9.99853	33.998	3.291	2.2578
Si-DLC	10.62175	36.128	3.504	2.4672

Table 2

Calculated deflection of proof ring for constant load test from SSRT curves.

Condition	Load (kgf)	Deflection (mm)
Elastic region	60	$63.5 \times 10^{-3}$
	100	$101.6 \times 10^{-3}$
Plastic region	147	$152.4 \times 10^{-3}$

were monitored continuously until fracture occurred. The load was applied at a constant strain rate of  $10^{-6} \text{ s}^{-1}$ . SSRT was conducted at freely-corroding, open-circuit potentials.

### 2.3. Constant load test (CLT)

The SCC test was performed using proof ring tester. From the SSRT stress–strain curve, we determined the load needed to deflect the ring to the desired value. The loads were transferred to the deflection to apply to the proof ring. CLT was conducted at freely-corroding, open-circuit potentials. During the deflection application, EIS test measurements were taken every 12 h up to 3 days.

### 2.4. Electrochemical measurements

All experiments were performed at 37 °C in 0.89 wt.% NaCl made with distilled water. The solution was thoroughly deaerated by bubbling high purity nitrogen gas for 2 h prior to specimen immersion and were continuously purged during the test. The exposed coating area was 5.12 cm<sup>2</sup>. The reference and counter electrodes were saturated calomel and pure graphite electrodes, respectively. Potentiodynamic test was conducted using an EG&G PAR 263 A for DC measurement. The EIS tests were conducted using a Zahner IM6e system with a commercial software program for the AC measurements. The amplitude of the sinusoidal perturbation was 20 mV. The frequency range was from 100 kHz to 1 mHz.

### 2.5. Coating analysis

After the constant load tests were completed, scanning electron microscopy (SEM) and X-ray photoelectron spectroscopy (XPS) were used to examine the surface of the specimens.

## 3. Results and discussion

In Fig. 1, the stress–strain–time curves of the Si-DLC and 316L SS specimens in the simulated body environment showed somewhat different behavior. The SSRT results for specimens are also given in

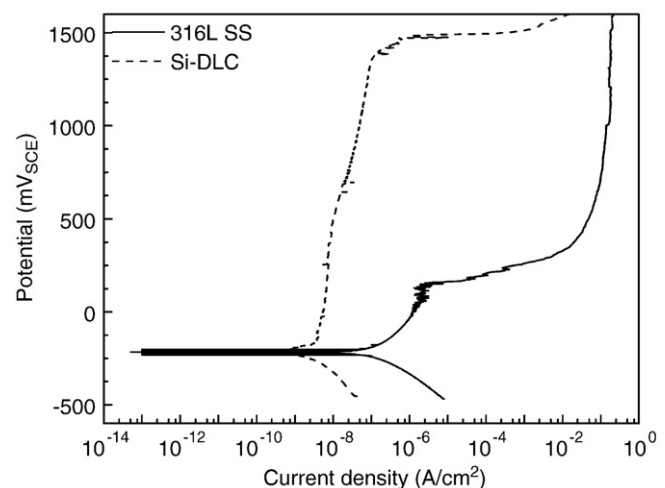


Fig. 2. Polarization curves for Si-DLC coated on 316L SS and 316L SS substrate in 0.89 wt.% NaCl electrolyte deaerated by bubbling high purity nitrogen gas at 37 °C.

**Table 3**  
Results of potentiodynamic polarization tests.

Specimen	$E_{corr}$ (mV)	$i_{corr}$ (nA/cm <sup>2</sup> )	$P_i$ (%)
Substrate	-223.46	129.20	-
Si-DLC	-215.63	1.56	98.79

**Table 1.** The difference between Si-DLC and 316L SS specimens clearly reflected reduction in elongation caused by the SCC process. The total strain of the Si-DLC specimen was 36%, compared to 34% for the substrate specimen, indicating more ductility of the Si-DLC coated steel compared to 316L SS substrate. This result was used to determine the necessary loads to calculate the deflected proof ring for CLT. As reference information about SSRT in **Table 2**, elastic loads were selected as 60, 100 kgf and plastic load was 147 kgf.

Potentiodynamic polarization curves for Si-DLC film and substrate are shown in **Fig. 2**. From polarization test results,  $P_i$ (%), the protective efficiency of the film, can be calculated by the following equation:

$$P_i(\%) = \left[ 1 - \left( \frac{i_{corr}}{i_{corr}^0} \right) \right] \times 100 \quad (1)$$

where  $i_{corr}$  and  $i_{corr}^0$  indicate the corrosion current density of the film and substrate, respectively [29]. The measured corrosion potential

( $E_{corr}$ ), corrosion current density ( $i_{corr}$ ), and protective efficiency ( $P_i$ ) are given in **Table 3**. The Si-DLC film was well passivated, with low passive current density and wide passive potential range. The high protective efficiency is closely related to the corrosion protection ability and durability of coating in 0.89 wt.% NaCl solution.

**Figs. 3 and 4** show Nyquist plots of the 316L SS and Si-DLC coated steel electrodes under stressed and unstressed conditions for 72 h. The EIS data for 316L SS substrate specimens among unstressed, elastic and plastic conditions were very different. However, the difference between elastic and plastic of Si-DLC specimens was not significant. The semicircle depression in the Nyquist diagram was attributed to the heterogeneity of the surface due to the stress effect. Most impedance data for Si-DLC films in corrosive media agreed with the equivalent circuit shown in **Fig. 5**, where  $R_s$  represents the solution resistance, and  $R_p$  the polarization resistance. In this case, the capacitor was replaced with a CPE to improve the fitting quality where CPE contained a double-layer capacitance ( $C$ ) and phenomenological coefficient ( $n$ ). The  $n$  value of a CPE indicates its meaning:  $n = 1$ , a capacitance;  $n = 0.5$ , a Warburg impedance;  $n = 0$ , a resistance and  $n = -1$ , an inductance [30]. In the present study,  $n$  was consistently maintained near 0.9, as a result of the deviation from ideal dielectric behavior which arose due to the heterogeneity of the surface both laterally and within the depth of the oxide film, which reflects the properties of the double layer.

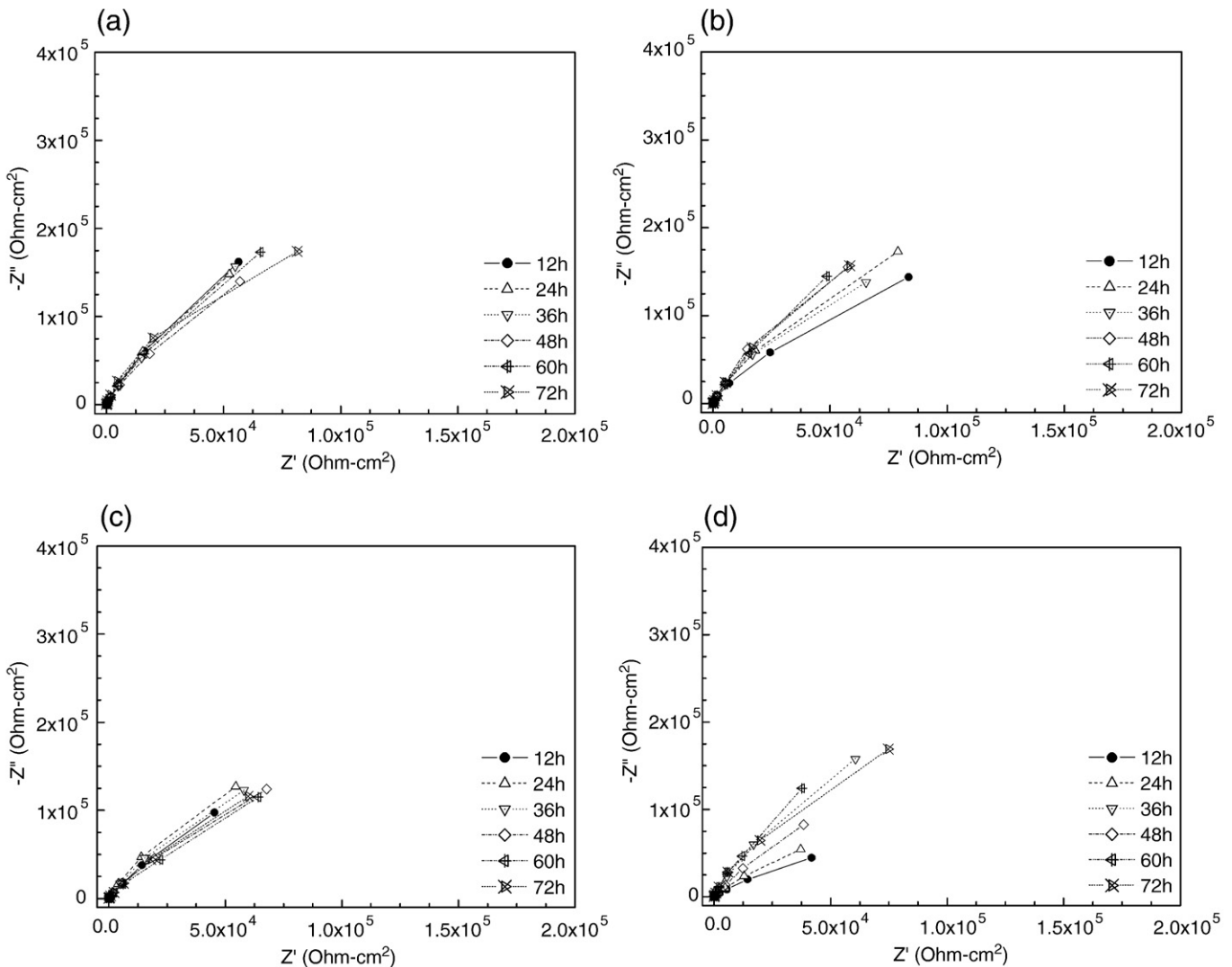


**Fig. 3.** Nyquist plots for 316L stainless steel specimens in simulated body environment: (a) unstressed condition; (b) and (c) elastic regions at 0.0025 and 0.0040 in., respectively; and (d) plastic region at 0.0060 in.

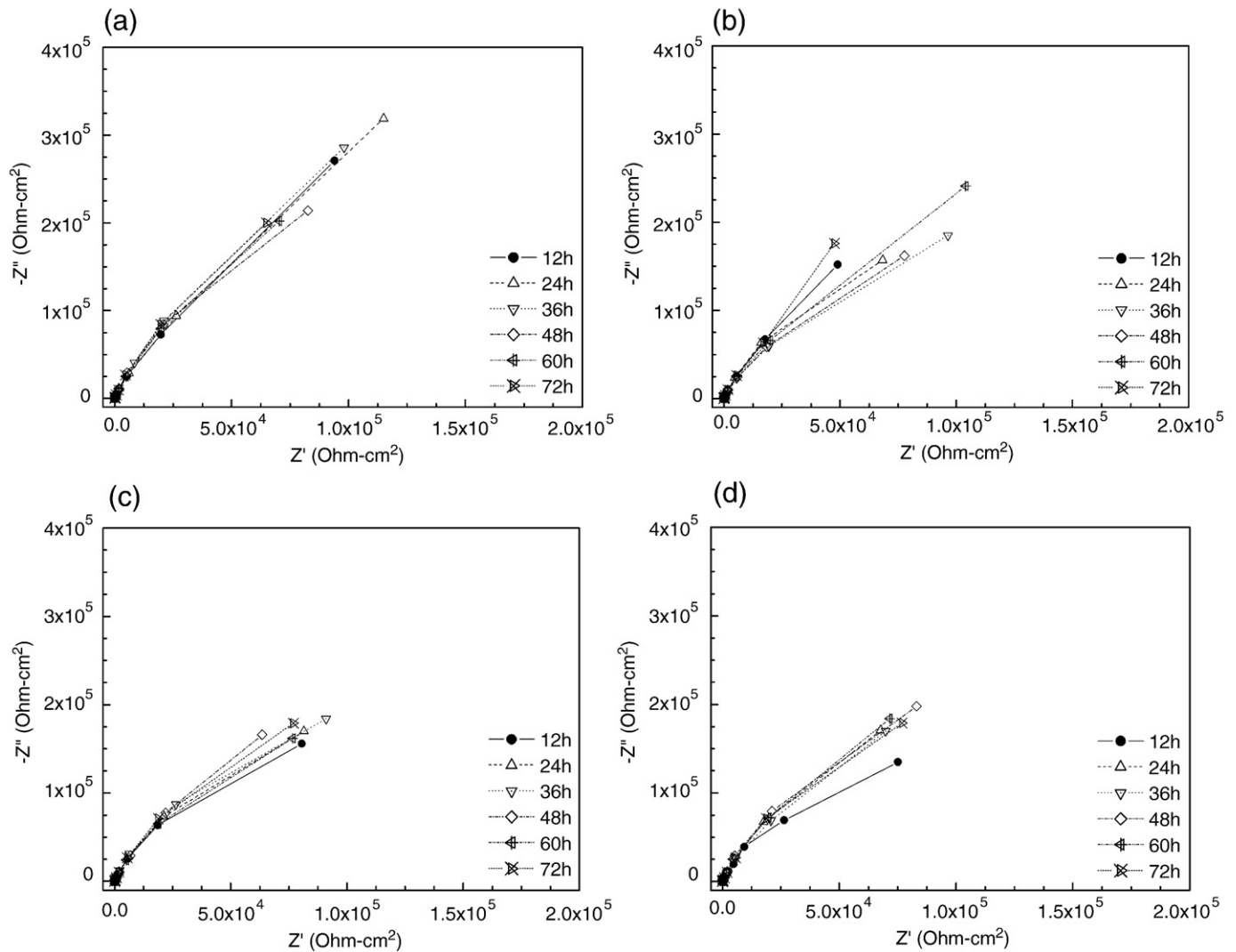


Fig. 4. Nyquist plots for Si-DLC specimens in simulated body environment: (a) unstressed condition; (b) and (c) elastic regions at 0.0025 and 0.0040 in., respectively; and (d) plastic region at 0.0060 in.

In Fig. 6, the coatings in all cases exhibited high polarization resistances ( $>10^6 \Omega \cdot \text{cm}^2$ ) during the immersion time, thereby indicating the low corrosion rates [31]. The absolute value of the impedance of substrate was clearly lower than those of coating. The initial increase in polarization resistance of Si-DLC coated steel under plastic stress might have been caused by the spontaneous passivity ability of the coating. It appears that film formation during electrolyte immersion maintained the high polarization resistance for both elastic and plastic regions. Even though the stress at plastic condition became more severe, the  $R_p$  was stable at high value. It reveals that the Si-DLC coating under plastic condition had high performance because of the enrichment of passive film.

It was found that the Si-DLC coating reduced the susceptibility of type 316L SS to SCC in the simulated body environment. The remarkable decrease of the polarization resistance of 316L SS substrate that occurred under different stressed conditions indicates that the susceptibility of 316L steel to SCC increased with an increase of the applied stress. However, no significant differences were observed in the polarization resistance of Si-DLC coated steel under stressed conditions. Therefore, the Si-DLC coated steel is less susceptible to SCC in this environment. EIS results indicate that the passive layer on the Si-DLC coating remained intact under stressed conditions. The applied stress appeared to have a

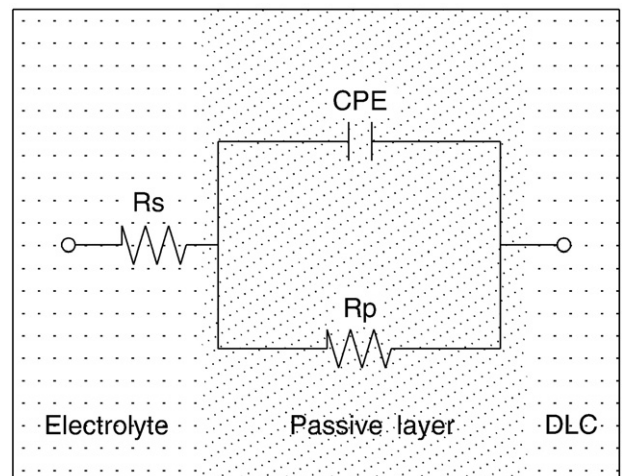
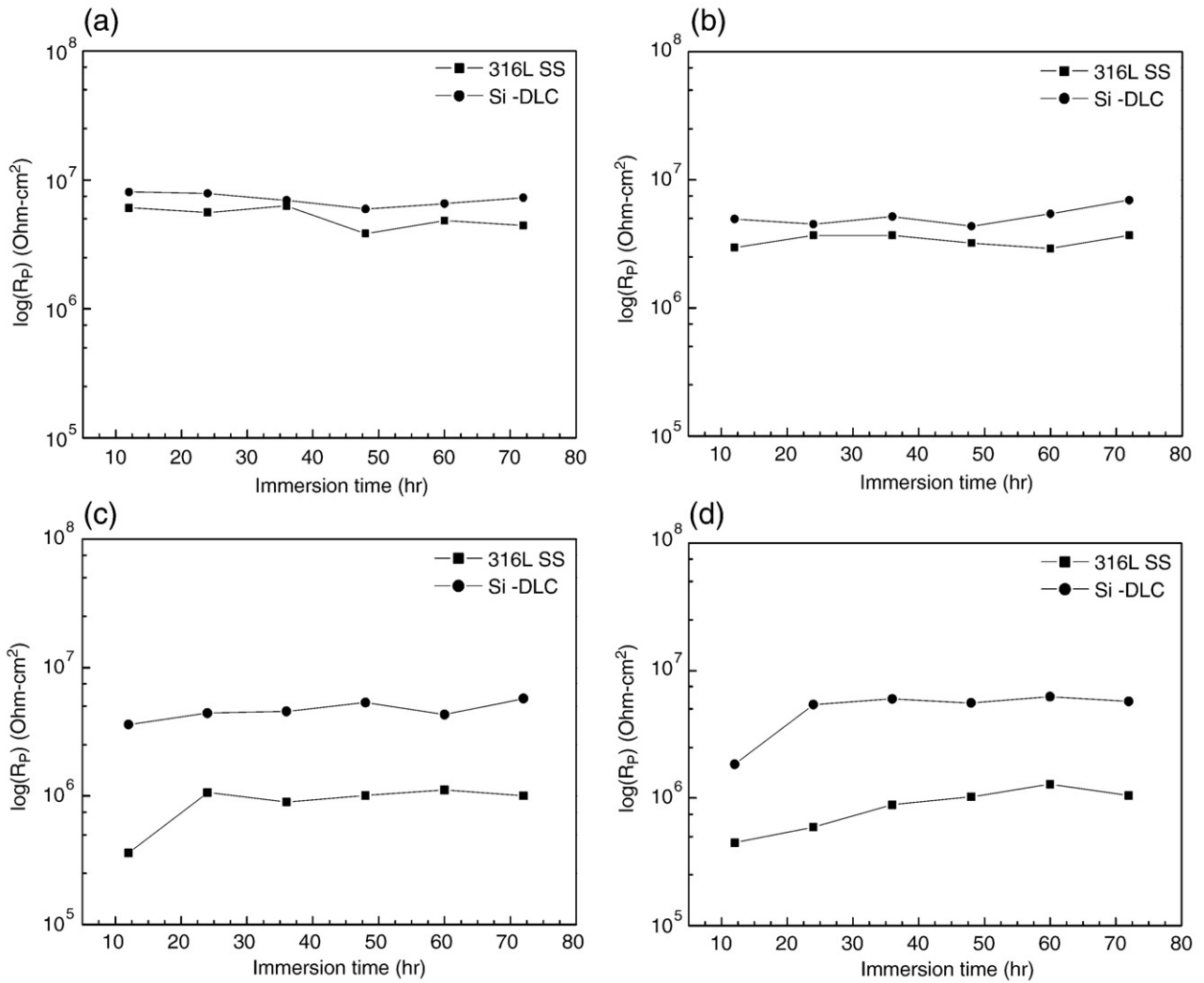


Fig. 5. Equivalent circuit to fit the electrochemical impedance spectroscopy (EIS) diagram of the Si-DLC specimen testing in the simulated body environment.



**Fig. 6.** Total resistance of 316L SS and Si-DLC on 316L SS as a function of time: (a) unstressed condition; (b) and (c) elastic regions at 0.0025 and 0.0040 in., respectively; and (d) plastic region at 0.0060 in.

negligible effect on the protective nature of the surface film. Although the plastic deformation ruptures the passive film, the rate of repassivation is as high as the rate of breakdown of passive film. The schematic figure of repassivation mechanism is given in Fig. 7. A model for the mechanism of the stressed damage of the DLC film can be described with the following three processes: (1) The first step is the formation of the passive film in 0.89 wt.% NaCl solution. (2) When the stress is applied to the specimen, the stress opened the film in front of its face with the

initial breakdown of passive film on Si-DLC film. It exceeds the critical stress that the film could be broken down, so as to release the stresses. (3) As soon as passive film was broken down, repassivation would be initiated due to the Si, which promotes repassivation of DLC film [26,27].

Surface films were evaluated by XPS measurement, with all results confirming the presence of silicon oxide in the Si-DLC surface after CLT (Fig. 8). However, it should be noted that the XPS analysis focused only on the surface data for the silicon oxide layer. The peaks at binding

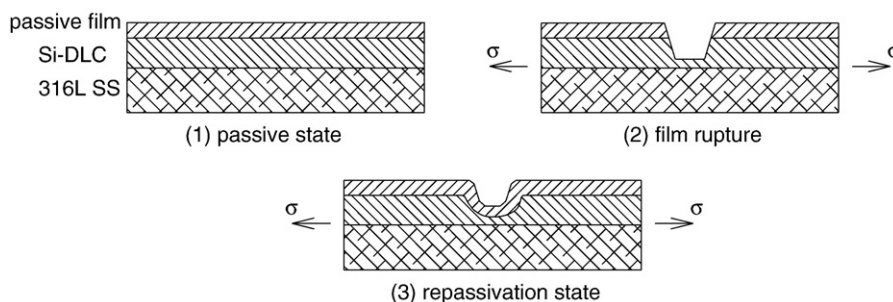


**Fig. 7.** Schematic figure of repassivation mechanism.

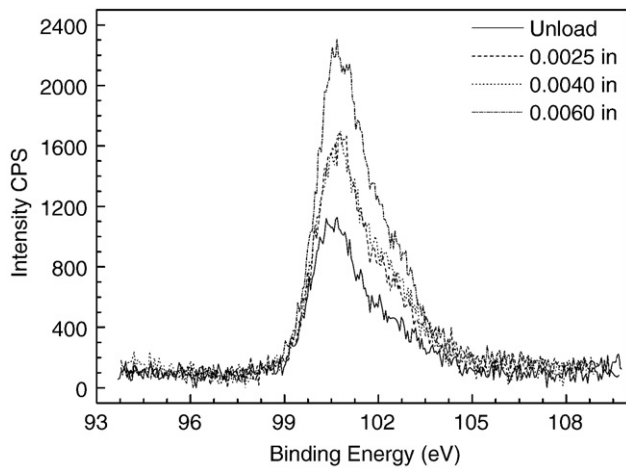


Fig. 8. Spectra of silicon oxide present on the Si-DLC surface as determined by XPS.

energies of 100.477, 101.973, and 103.407 eV represented  $\text{SiO}_x$  [32,33] and those of 102.387, 102.419, and 102.494 eV represented Si–C–O compound [34,35]. The composition of the top layer of the oxide film, as estimated by quantitative analysis in Table 4, was Si–C–O compound formed from silicon during the stress application. In addition, this figure also shows that the silicon oxide containing Si–C–O compound was enriched with the applied load due to the silicon migration outwards through the passive film.

The surface after CLT was examined by SEM. Fig. 9 shows numerous coating cracks on the specimen surface with vertical crack growth parallel in the film and rising density with increasing stress. It is noteworthy that the absence of any pitting between the cracks indicated repassivation and film growth.

#### 4. Conclusions

1. The SSRT confirmed the higher ductility of the Si-DLC coated steel compared to uncoated steel. The Si-DLC coated steel is less susceptible to SCC than 316L SS.
2. The Si-DLC coating under the plastic load had much higher polarization resistance than 316L SS, i.e., the applied plastic stress did not appear to influence the protective nature of the film.
3. The XPS test results showed that the Si-DLC films improved the corrosion resistance of steel under the stressed condition due to the presence of the silicon oxide layer on the Si-DLC film.

Table 4

Quantitative analysis of Si 2p obtained by XPS after test.

Load	Name	Concentration (%)	Area	Position	Height
Unload	Si 2p <sub>3/2</sub> ( $\text{SiO}_x$ )	1.201	1547.267	100.477	937.779
	Si 2p <sub>3/2</sub> ( $\text{SiO}_x$ )	0.527	679.379	101.973	340.568
	Si 2p <sub>3/2</sub> ( $\text{SiO}_x$ )	0.224	288.087	103.407	127.351
60 kgf	Si 2p <sub>3/2</sub> ( $(\text{C}_6\text{H}_5)_3\text{Si}$ )	1.400	2561.758	100.678	1456.962
	Si 2p <sub>3/2</sub> (Si–C–O compound)	0.545	997.195	102.494	484.636
100 kgf	Si 2p <sub>3/2</sub> ( $(\text{C}_6\text{H}_5)_3\text{Si}$ )	1.486	2519.487	100.650	1409.378
	Si 2p <sub>3/2</sub> (Si–C–O compound)	0.723	1225.307	102.419	595.499
147 kgf	Si 2p <sub>3/2</sub> ( $(\text{C}_6\text{H}_5)_3\text{Si}$ )	1.923	3495.648	100.694	1989.930
	Si 2p <sub>3/2</sub> (Si–C–O compound)	0.877	1593.551	102.387	774.465

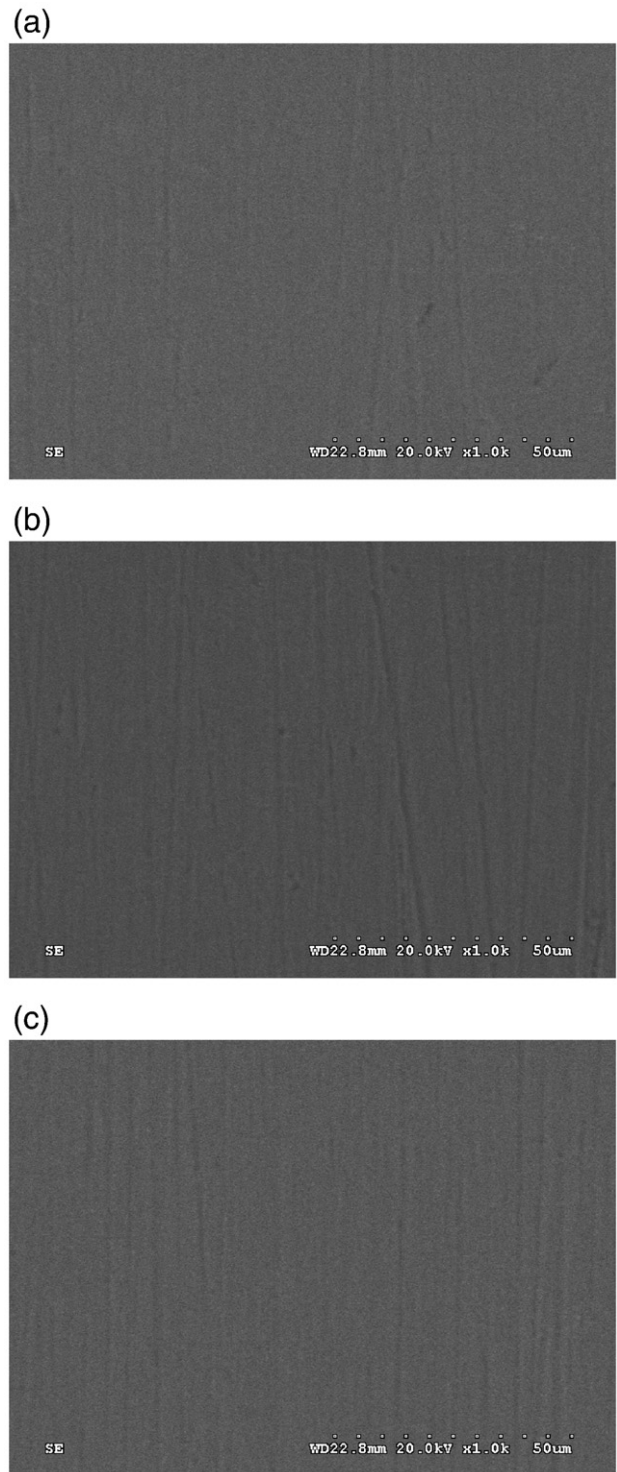


Fig. 9. SEM photographs of Si-DLC after CLT test: (a) and (b) elastic regions at 0.0025 and 0.0040 in., respectively; and (c) plastic region at 0.0060 in.

4. From the typical SEM images after CLT, the surface of Si-DLC coated steel showed no active path at the cracks, indicating repassivation of the film.

#### References

- [1] O.F. Bertrand, R. Sipehia, R. Mongrain, J. Rodés, J.C. Tardif, L. Bilodeau, C. Gilles, M.G. Bourassa, JACC 32 (1998) 562.
- [2] R. Barbucci, M. Santin, L. Ambrosio, A.W. Lloyd, S.P. Denyer, Integr. Biomater. Sci. (2002) 425.
- [3] L.K. Keeper, Nat. Mater. 2 (2003) 357.

- [4] M.M. Mazumder, S. De, S. Trigwell, N. Ali, M.K. Mazumder, J.L. Mehta, J. Biomater. Sci., Polymer. Ed. 14 (2003) 1351.
- [5] R. Venugopalan, J. Biomed. Mater. Res. 48 (1999) 829.
- [6] Y.P. Kathuria, Int. J. Cardiol. 119 (2007) 380.
- [7] G.K. Riepe, C.K. Heintz, E.K. Kaiser, N.K. Chakfe, M.K. Morlock, M.K. Delling, H.K. Imig, Eur. J. Vasc. Endovasc. Surg. 24 (2002) 117.
- [8] C. Heintz, G. Riepe, L. Birken, E. Kaiser, N. Chakfe, M. Morlock, G. Delling, H. Imig, J. Endovasc. Ther. 8 (2001) 248.
- [9] C. Trepanier, T.K. Leung, M. Tabrizian, L.H. Yahia, J.G. Bienvenu, J.F. Tanguay, D.L. Piron, L. Bilodeau, J. Biomed. Mater. Res. 48 (1999) 165.
- [10] B. Thierry, M. Tabrizian, O. Savadogo, L.H. Yahia, J. Biomed. Mater. Res. 49 (2000) 88.
- [11] S.N. David Chua, B.J. Mac Donald, M.S.J. Hashmi, J. Mater. Process. Technol. 120 (2002) 335.
- [12] C. Rogers, D.Y. Tseng, J.C. Squire, E.R. Edelman, Circ. Res. 84 (1999) 378.
- [13] C. Dumoulin, B. Cochelin, J. Biomech. 33 (2000) 1461.
- [14] F. Etave, G. Finet, M. Boivin, J.C. Boyer, G. Rioufol, G. Thollet, J. Biomech. 34 (2001) 1065.
- [15] W.D. Whitcher, Comput. Struct. 64 (1997) 1005.
- [16] R.L.W. Messer, J. Mickalonis, Y. Adam, W.Y. Tseng, J. Biomed. Mater. Res. Part B: Appl. Biomater. 76B (2006) 273.
- [17] D.A. Jones, Principles and Prevention of Corrosion, 2nd, Prentice Hall, Singapore, 1997, p. 235.
- [18] R.W. Bosch, F. Moons, J.H. Zheng, W.F. Bogaerts, Corrosion 67 (2001) 532.
- [19] K. Darowicki, J. Orlikowski, A. Arutunow, W. Jurczak, J. Electrochem. Soc. 154 (2007) C74.
- [20] D.H. Hur, Corrosion 59 (2003) 203.
- [21] R. Oltra, M. Keddad, Corros. Sci. 28 (1988) 1.
- [22] Y.S. Choi, J.G. Kim, Mat. Sci. Eng. A 333 (2002) 336.
- [23] H.W. Choi, K.R. Lee, R. Wang, K.H. Oh, Diam. Relat. Mater. 15 (2006) 38.
- [24] A.A. Ogwu, T. Coyle, T.I.T. Okpalugo, P. Kearney, P.D. Maguire, J.A.D. McLaughlin, Acta Mater. 51 (2003) 3455.
- [25] E.H.A. Dekempeneer, R. Jacobs, J. Smeets, J. Meneve, L. Eersels, B. Blanpain, J. Roos, D.J. Oostra, Thin Solid Films 217 (1992) 56.
- [26] H.G. Kim, S.H. Ahn, J.G. Kim, S.J. Park, K.R. Lee, Diam. Relat. Mater. 14 (2005) 35.
- [27] H.G. Kim, S.H. Ahn, J.G. Kim, S.J. Park, K.R. Lee, Thin Solid Films 475 (2005) 291.
- [28] NACE Standard TM0177-96. Laboratory testing of metals for resistance to specific forms of environmental cracking in H<sub>2</sub>S environments, NACE, Houston 1996.
- [29] T. Daiki, H. Reiko, A. Kunitsugu, Corros. Sci. 43 (2001) 1589.
- [30] L.V. Leaven, M.N. Alias, R. Brown, Surf. Coat. Technol. 53 (1992) 25.
- [31] H. Alanyali, R.M. Souto, Corrosion 59 (2003) 851.
- [32] S.S. Chao, Y. Takagi, G. Lucovsky, P. Pai, R.C. Custer, J.E. Tyler, J.E. Keem, Appl. Surf. Sci. 26 (1986) 575.
- [33] H. Du, R.E. Tressler, K.E. Spear, C.G. Pantano, J. Electrochem. Soc. 136 (1989) 1527.
- [34] J.A. Gardella, R.L. Chin, S.A. Ferguson, M.M. Farrow, J. Electron. Spectrosc. Relat. Phenom. 8 (1976) 343.
- [35] C.D. Wagner, D.E. Passoja, H.F. Hillery, T.G. Kinisky, H.A. Six, W.T. Jansen, J.A. Taylor, J. Vac. Sci. Technol. 21 (1982) 933.